α-Melt-Mediated Crystallization of 1-Palmitoyl-2-Oleoyl-3-Stearoyl-*sn*-Glycerol

Ph. Rousset* and M. Rappaz

Département des Matériaux, Ecole Polytechnique Fédérale de Lausanne, MX-G, CH-1015 Lausanne, Switzerland

ABSTRACT: The α-melt-mediated crystallization of 1-palmitoyl-2-oleoyl-3-stearoyl-*sn*-glycerol (POS) has been investigated by differential scanning calorimetry (DSC), combined with polarized-light microscopy. Starting from a completely liquid state, the melt was first cooled down and maintained at a temperature, T_1 , during a time, t_1, where the α-phase formed. Then it was heated to a temperature, T_2, above the melting point of α for isothermal solidification into a solid phase, which was identified as δ. Based upon DSC solidification peaks, the time–temperature–transformation (TTT) diagram of POS was constructed for these solidification conditions and was compared with the TTT diagram of direct crystallization from the melt. The α-melt-mediated solidification showed accelerated kinetics of the δ-phase. The effects of T_1 and t_1 were also studied: at short t_1, crystallization was faster with a decreasing value of T_1, whereas the opposite trend was observed for a longer plateau at T_1. These tendencies were interpreted in terms of three competing phenomena: the density of δ-nuclei that can form during the plateau at T_1, α-δ solid-state transformation, and memory effects of molecule arrangements in the α-remelted phase.
JAOCS 74, 693–697 (1997).

KEY WORDS: Cocoa butter, crystallization, DSC, kinetics, polarized-light microscopy, polymorphism, POS, solidification, spherulite, triacylglycerol.

Tempering is an important stage in the manufacturing of chocolate to obtain the desired phase V of cocoa butter (1). During this processing stage, the completely liquid cocoa butter is first brought to a temperature at which nuclei from both phases IV and V form. The mixture is then heated to a temperature where the seeds of form IV are remelted. After these two steps, a sufficient number of nuclei of phase V are present in the melt to allow solidification in the desired form during the final cooling in the mold (2–6). By this process, the crystallization kinetics of phase V are much faster than for direct crystallization from the melt at the same temperature (2–4).

The parameters of the tempering process depend on the characteristics of the cocoa butter and of the other components used, but the mechanisms responsible for the crystallization kinetics are not fully understood. To improve knowledge of this so-called melt-mediated crystallization, a series of experiments by differential scanning calorimetry (DSC), coupled with polarized light microscopy (PLM), has been carried out on 1-palmitoyl-2-oleoyl-3-stearoyl-*sn*-glycerol (POS). Koyano and coworkers (7,8) already observed the sharp increase in solidification rate and the appearance at lower temperature of more stable phases for melt-mediated crystallization of 1,3-dipalmitoyl-2-oleoyl-*sn*-glycerol (POP), POS, and 1,3-distearoyl-2-oleoyl-*sn*-glycerol (SOS). However, their main aim was to study the occurrence of polymorphism of each triacylglycerol (TAG) as a function of solidification conditions. They put forward some hypotheses that could explain the faster kinetics of melt-mediated crystallization. In the present investigation, the effects of temperature and duration of a first isothermal plateau on the crystallization kinetics at a higher temperature were investigated. Based upon the DSC peaks and morphologies of the crystals, some conclusions are drawn regarding the mechanisms involved during melt-mediated crystallization.

MATERIALS AND METHODS

POS (purity of 99%) was purchased from Larodan Fine Chemicals AB (Malmö, Sweden). Crystallization kinetics of POS were investigated by DSC (Mettler FP900, Greifensee, Switzerland), coupled with *in situ* polarized-light microscopic observations. The FP900 DSC apparatus is equipped with a window for observation and glass pans for the reference and sample. This allows direct visualization under polarized light of the evolution of growing crystals and simultaneous measurement of the DSC peaks. The samples had masses between 0.5 and 2 mg.

Two different solidification procedures were used. (i) Direct solidification: The sample was maintained in the liquid state at 100°C for 3 min. It was then cooled quickly (10°C/min) to the desired temperature T_2 and allowed to crystallize isothermally at this temperature. (ii) Melt-mediated crystallization: Starting from the same liquid state, the melt was cooled quickly (10°C/min) to a first plateau T_1 ($T_1 < T_2$) and maintained at this temperature during a period t_1 (see Fig. 1). At T_1, the most metastable phase (i.e., α) formed if t_1 was sufficiently long (7,9). The sample was then heated quickly (10°C/min) to T_2 , above the melting point of α. The α-phase

---

*To whom correspondence should be addressed.
E-mail: rousset@lmph.dmx.epfl.ch.

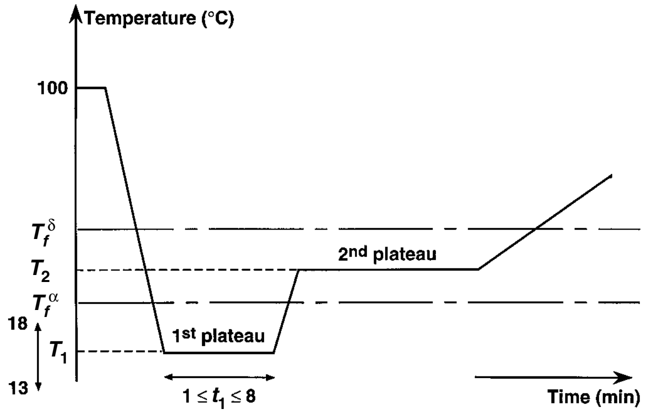

FIG. 1. Temperature path used for the α-melt-mediated crystallization of 1-palmitoyl-2-oleoyl-3-stearoyl-*sn*-glycerol.

remelted (if it had formed), and the mixture was allowed to resolidify isothermally at this temperature.

At the end of both solidification procedures, the fully solid samples were heated at 5°C/min to measure the temperature and the latent heat of fusion of the final phase(s) formed. These data were used to identify these phases by comparison with results previously obtained by Arishima *et al.* (10).

When not specified, the parameters of the first plateau for the melt-mediation experiments were T_1 = 15°C and t_1 = 4 min. They allowed the liquid to be completely transformed into the α-phase (9).

For both direct and melt-mediated crystallization experiments, the crystallization kinetics on the second plateau at T_2 were studied. The evolution of the volume fraction of solid, $f_s(t)$, which formed at T_2, was obtained by numerical integration of the DSC exothermal peaks of solidification, after correction for the baseline. From the evolution of $f_s(t)$ on this second plateau, two parameters were calculated for further analysis: the time of onset, t_{onset}, and the time of finish, t_f, of the transformation, which correspond to $f_s(t_{\text{onset}})$ = 1% and $f_s(t_f)$ = 99%; t_{onset} and t_f were used to characterize the kinetics of the transformation.

Time–temperature–transformation (TTT) diagrams, which represent phase transformation kinetics under isothermal conditions, were also constructed, as previously described (9): For each temperature of solidification, t_{onset} and t_f of the phase transformation were reported on the diagram, thus delimiting the domain of liquid–solid crystallization.

The curves $f_s(t)$ were further analyzed in terms of an Avrami-type law (11,12). By assuming that spherulites were growing in an isothermal melt, the volume fraction of solid could be described as:

$$f_s(t) = 1 - \exp\left[-\int_0^t \dot{n}(\tau)\tfrac{4}{3}\pi G^3 (t-\tau)^3 d\tau\right] \qquad [1]$$

where $\dot{n}(\tau)$ is the nucleation rate at time τ and is unknown. G is the growth rate, assumed to depend only on the temperature, here determined by the direct observation of the evolution of the grain radius with time. The time t appearing in Equation 1 was not measured after the beginning of the isothermal plateau but was shifted by a time of induction, t_{ind}. This time is necessary to establish a stationary embryo population (13). Making the assumption of a constant nucleation rate, $\dot{n}$, the measured $f_s(t)$-curves were fitted with Equation 1, taking $\dot{n}$ and t_{ind} as adjustable parameters.

RESULTS AND DISCUSSION

TTT diagram of POS. Figure 2 shows the TTT diagram of POS, measured during direct (continuous curves) and α-melt-mediated crystallization (dotted curves). Equilibrium melting temperatures of the α- and δ-phases are also reported (dashed horizontal lines). The filled and open symbols correspond to t_{onset} and t_f measured for each temperature T_2.

As already reported by Rousset and Rappaz (9), direct crystallization of POS can occur under two different crystallographic phases in the temperature interval 15–21°C: below 18°C, the α-phase forms quite rapidly, whereas above 19°C, the δ-phase crystallizes at a much slower rate. For both phases, an increase in the undercooling (i.e., the departure from the corresponding equilibrium melting point), ΔT, leads to faster transformation kinetics.

The α-melt-mediated crystallization kinetics of POS was investigated in the temperature interval of 20–27°C (dotted curves): In these experiments, only the δ-phase formed during the second isothermal plateau. The kinetics were again faster (i.e., t_{onset} and t_f shorter) as the temperature of this plateau was lowered, but more important, the liquid–solid transformation was much faster than that of direct crystallization.

The morphologies of the δ-crystals formed at 20 or 21°C during the two solidification procedures were also quite different. In direct crystallization, quite large spherulites (average size about 50 μm) were observed, whereas the microstructure obtained during the second plateau of α-melt-

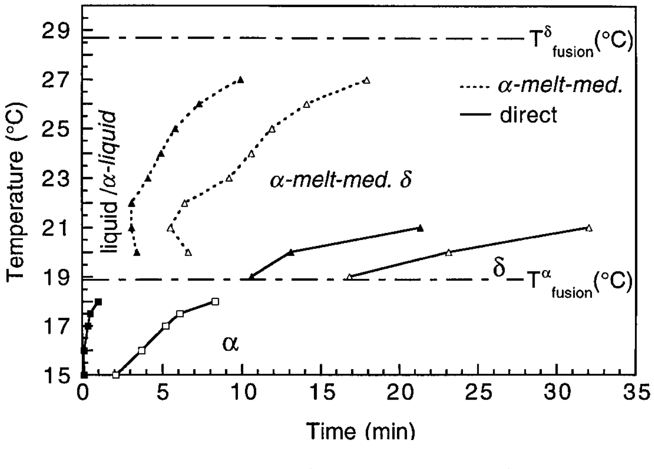

FIG. 2. Time–temperature–transformation diagram of 1-palmitoyl-2-oleoyl-3-stearoyl-*sn*-glycerol for direct and α-melt-mediated (melt-med.) crystallization. Filled and open symbols correspond to the time of onset and the time of finish of the transformation, whereas squares and triangles are used for the α- and δ-phases, respectively.

mediated crystallization was fine and the grain size could hardly be estimated (lower than 5–10 µm).

The results obtained in the present investigation were compared with those reported by Koyano *et al.* (7) (see Fig. 3). These authors measured with a photosensor the intensity of the polarized light passing through a specimen undergoing liquid–solid transformation. From this signal, they deduced the start time of the transformation at different temperatures under direct and α-melt-mediated crystallization conditions. As in the present investigation (Fig. 2), the first plateau of the α-melt-mediated crystallization was also made at 15°C for about 5 min. Because Koyano *et al.* only detected the beginning of the transformation, only the times of onset of direct and α-melt-mediated crystallization are compared in Figure 3. In the temperature interval 20–24°C, Koyano *et al.* measured slightly shorter times of onset during direct solidification and identified the formation of β′ instead of δ for our experiments. For α-melt-mediated crystallization, with a second isothermal plateau in the interval 20–27°C, they obtained times of onset very close to the present results, but again they identified β′ formed rather than δ. These differences show the high sensitivity of the results to the experimental conditions used, the nucleation kinetics probably being the most influenced by the external conditions. For example, it was demonstrated that the use of aluminum or glass pans in DSC experiments could substantially modify the crystallization kinetics of POS (9).

Effect of the parameters of the first plateau. For a better understanding of the reasons for the accelerated kinetics of δ during α-melt-mediated crystallization, the temperature T_1 and the time t_1 of the first plateau (where α forms) were varied in a series of experiments, while T_2 was kept constant at 21°C (see Fig. 1). T_1 was changed in the interval 13–18°C, while t_1 was varied between 1 and 8 min. Under such conditions, the phase that formed at T_2 was always identified as δ.

The effects of the two parameters T_1 and t_1 on the time of onset and the duration (i.e., $t_f - t_{\text{onset}}$) of the formation of δ on the second plateau are summarized in Figures 4A and B, respectively. Keeping t_1 constant, the times of onset measured at various T_1 were fitted with a linear regression. Two different trends can be observed (Fig. 4A): At small time t_1 (1 or 2 min), as temperature T_1 is increased, t_{onset} increases, i.e., the liquid–δ-phase transformation starts later. The opposite trend is observed for longer plateaus ($t_1 \geq 4$ min), i.e., the formation of δ occurs earlier as T_1 is increased. Furthermore, for small t_1 values (1 or 2 min), the duration of δ-crystallization is markedly longer when the temperature T_1 is increased, whereas, for longer t_1 (≥4 min), it is not very sensitive to variations of T_1 (Fig. 4B).

The dependence of crystallization kinetics of δ on parameters T_1 and t_1 of the first isothermal plateau is accompanied by a change in the morphology of δ-crystals (Fig. 5). At small values of the product $T_1 \cdot t_1$, the δ spherulites are well defined and clearly show a Maltese cross at their center (see in Fig. 5B the microstructure observed under polarized light after a

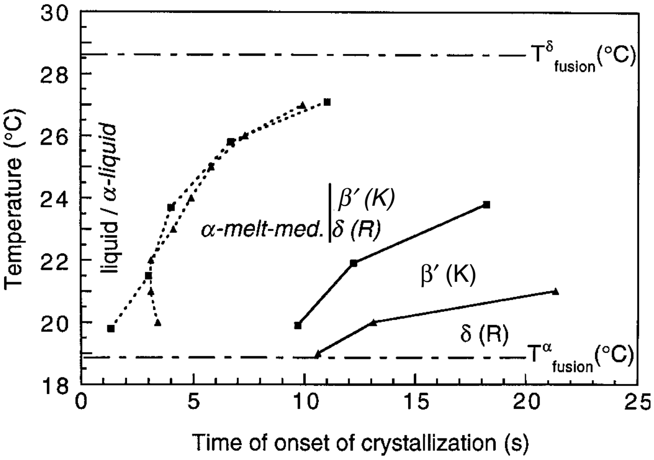

FIG. 3. Comparison of the times of onset measured by Koyano (K) (Ref. 2) and in the present study (R) for direct and a-melt-mediated crystallization. Key: —▲—, direct (R); —■—, direct (K); ---▲---, α-melt-mediated (*R*); ---■---, α-melt-mediated (*K*). See Figure 2 for abbreviated wording explanation.

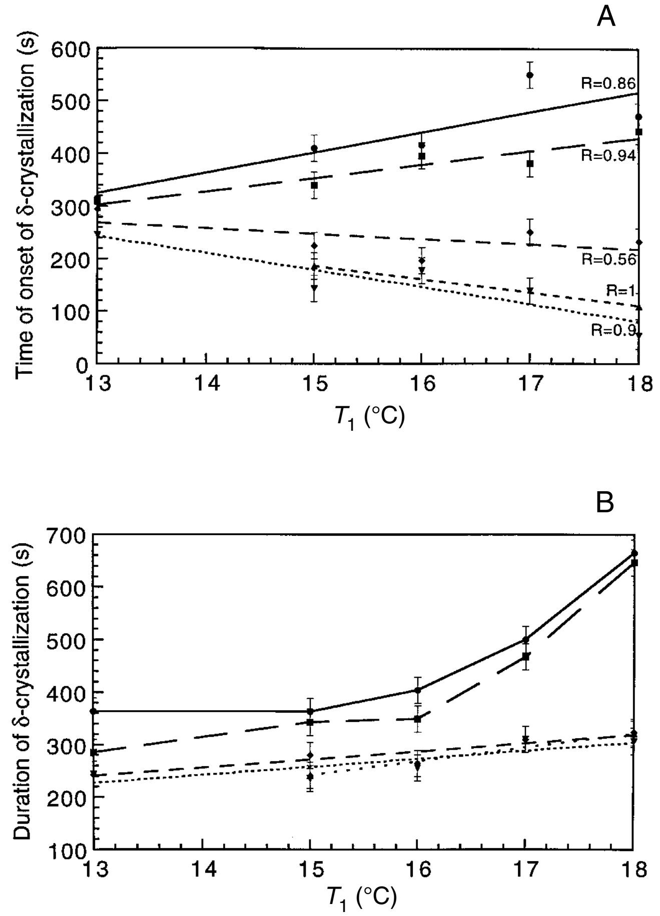

FIG. 4. Time of onset (A) and duration (B) of δ-crystallization as a function of temperature T_1 and time t_1 of the first isothermal plateau (R is the regression coefficient of each of the linear fits). Key: —●—, t_1 = 1 min; ——■——, t_1 = 2 min; – –◆– –, t_1 = 4 min; --▲--, t_1 = 6 min; ---▼---, t_1 = 8 min. *R* is the regression coefficient of each of the linear fits, and the vertical bars are estimated errors.

FIG. 5. Morphology map of δ-crystals as a function of temperature T_1 and time t_1 of the first isothermal plateau. The micrographs (A) and (B) correspond to the top right and bottom left conditions of the morphology map, respectively.

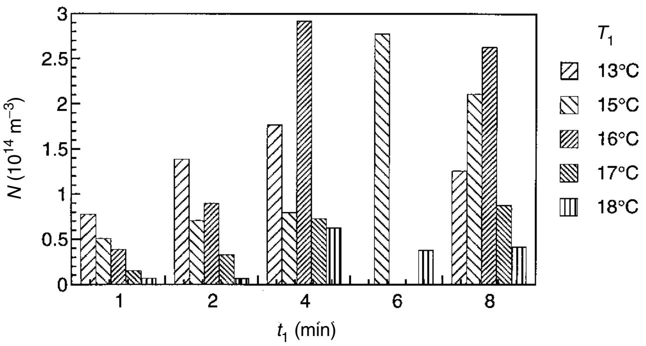

FIG. 6. Density of grains N deduced from the Avrami analysis as a function of temperature T_1 and time t_1 of the first isothermal plateau.

first isothermal plateau at 13°C for 1 min). In the upper right corner of the microstructure map (larger values of $T_1 \cdot t_1$), an increasing number of fuzzy, irregular-shaped spherulites of δ are observed (see the morphology after a first isothermal plateau at 18°C for 8 min in Fig. 5A). The microstructure map, shown in the center of Figure 5, gives an estimated percentage of fuzzy crystals observed under PLM.

For each experiment, the analysis method of Equation 1 was applied to fit the measured $f_s(t)$ with t_{ind} and $\dot{n}$ as adjustable parameters. The growth rate G appearing in this equation was estimated to be 0.08 ± 0.02 µm/s (average value of about 50 spherulites) at 21°C. The density of spherulites, N, calculated from integration of the adjusted $\dot{n}$, is plotted as a function of t_1 and T_1 in Figure 6.

The faster crystallization of δ-phase during α-melt-mediated solidification, as compared with direct crystallization from the melt, can be analyzed in terms of three competing mechanisms: (i) Formation of more nuclei at lower temperatures. More nuclei of the δ-phase can directly form from the melt if the sample is brought to a lower temperature. Nucleation theory states that the nucleation rate from an equilibrium distribution of embryos is enhanced as the temperature is decreased. Furthermore, the induction time required to establish such an equilibrium distribution at T_2 will be decreased once the temperature is increased from the lower temperature T_1. (ii) Transformation of small α-regions into δ (solid-state transformation). Although an endothermic peak, associated with the melting of the α-phase, is clearly measured with the DSC apparatus during heating from T_1 to T_2, this does not rule out solid-state transformation (exothermic reaction) of small regions (clusters) of α into δ. Because α is metastable, this direct transformation can occur during the first plateau and will be enhanced if T_1 is close to the melting point of the α-phase. (iii) "Memory" effect of the melt (14,15). Once the liquid has already been solidified into the metastable phase α, the POS molecules are not completely disordered after melting, and the δ-phase can benefit from this prearrangement of the molecules.

As a result of the Avrami analysis, it has been found that the experimental $f_s(t)$ curves can be described well by Equation 1 when the first isothermal plateau is short (i.e., small t_1). This good agreement is also consistent with the calculated grain densities shown in Figure 6. The density of δ-grains decreases with increasing temperature T_1. This means that, when there is insufficient time to grow the α-phase completely during the first isothermal plateau, the faster kinetics of the δ-phase during the second plateau are primarily associated with mechanism (i). Indeed, a higher density of grains also means faster kinetics because the solid–liquid interface is more fragmented. This finding is also consistent with spherulite morphology observed (Fig. 5B). The grains have a well-defined Maltese cross appearance, as for direct crystallization from the melt (9), because the melt did not have time to presolidify during the first isothermal plateau.

On the contrary, at high duration t_1, the experimental $f_s(t)$ curves cannot be fitted well with Equation 1, and the final density of grains seems to be an erratic function of T_1 (see Fig. 6). The time of onset for δ-crystallization is reduced when T_1 is increased (Fig. 4A), but the duration of crystallization, although shorter, is almost independent of T_1 (Fig. 4B). Furthermore, the spherulites have a fuzzy appearance (Fig. 5A). All these findings support the predominance of the memory effect mechanism (iii) mentioned above, although the two others could play a role. The molecules in the melt, after the α-phase has been remelted, keep some kind of arrangement and thus the grains can nucleate faster, but the spherulites do not grow regularly (fuzzy appearance) as compared with growth from randomly oriented molecules. The time of onset decreases when T_1 is increased because nuclei of δ can form more readily from α when the temperature is close to the melting point of α. This "α-melt-mediated" nucleation apparently dominates "direct" nucleation of δ from the melt encountered at short t_1. However, the density of nuclei does not seem to change drastically as a function of T_1 because the crystallization duration is shorter but almost independent of T_1 (Fig. 4B).

To summarize, the first plateau during α-melt-mediated crystallization of POS accelerates subsequent solidification of δ owing to two main mechanisms: first, the δ-nuclei formed directly from the melt are more numerous and appear more quickly because of the passage at T_1 . Second, if this first plateau is sufficiently long for α to form, it seems that some structure of α remains in the melt at the beginning of the second plateau ("memory effect") and that some α embryos retransform into δ, which will dramatically accelerate the formation of δ nuclei.

ACKNOWLEDGMENTS

The authors thank the Commission pour la Technologie et l'Innovation (CTI), Bern, Switzerland, and the Nestlé Research Center, Verschez-les-Blanc, Switzerland, for their financial support (CTI project 2944.1). The encouragement of Dr. Löliger and helpful discussions with Dr. C. Bertoli and Dr. E. Minner, from Nestlé Research Center, are also gratefully acknowledged.

REFERENCES

1. Talbot, G., Chocolate Temper, in *Industrial Chocolate Manufacture and Use*, edited by S.T. Beckett, Blackie Academic & Professional, Glasgow, 1994, pp. 156–166.
2. Ziegleder, G., Kristallisation von Schokoladenmassen, Teil I, Kristallkeimbildung, *Zucker Süsswaren Wirtschaft 5*:165–168 (1988).
3. Ziegleder, G., K. Becker, M. Baumann, and O. Rosskopf, Kristallisation von Schokoladenmassen, Teil II, Vorkristallisation und Temperiergrad, *Ibid. 7*:238–243 (1988).
4. Ziegleder G., and M. Kegel, Kristallisation von Schokoladenmassen, Teil III, DSC-Messung der Kühlungkristallisation, *Ibid. 10*:338–342 (1989).
5. Hausmann, A., H. Tscheuschner, I. Tralles, and H. Zscheile, Einfluss der Abkühlbedingungen auf die Auskristallisation der Schokolade, *Ibid. 2*:65–74 (1993).
6. Koyano, T., I. Hachiya, and K. Sato, Fat Polymorphism and Crystal Seeding Effects on Fat Bloom Stability of Dark Chocolate, *Food Structure 9*:231–240 (1990).
7. Koyano, T., I. Hachiya, T. Arishima, N. Sagi, and K. Sato, Polymorphism of POS. II. Kinetics of Melt Crystallization, *J. Am. Oil Chem. Soc. 68*:716–718 (1991).
8. Koyano, T., I. Hachiya, T. Arishima, K. Sato and N. Sagi, Polymorphism of POP and SOS. II. Kinetics of Melt Crystallization, *Ibid. 66*:675–679 (1989).
9. Rousset, Ph., and M. Rappaz, Crystallization Kinetics of the Pure Triacylglycerols Glycerol-1,3-Dipalmitate-2-Oleate, Glycerol-1-Palmitate-2-Oleate-3-Stearate, and Glycerol-1,3-Distearate-2-Oleate, *Ibid. 73:*1051–1057 (1996).
10. Arishima, T., N. Sagi, H. Mori, and K. Sato, Polymorphism of POS. I. Occurrence of Polymorphic Transformation, *Ibid. 68:*710–715 (1991).
11. Avrami, M., Kinetics of Phase Change I, *J. Chem. Phys. 7:*1103–1112 (1939).
12. Avrami, M., Kinetics of Phase Change II, *Ibid. 8:*212–224 (1940).
13. Kenny, J., A. Maffezzoli, and L. Nicolais, A New Kinetic Model for Polymer Crystallization Derived by Calorimetric Analysis, *Thermochim. Acta 227:*83–95 (1993).
14. Hernqvist, L., On the Structure of Triglycerides in the Liquid State and Fat Crystallization, *Fette Seifen Anstrichm. 8*:297–300 (1984).
15. Larsson, K., On the Structure of the Liquid State of Triglycerides, *J. Am. Oil Chem. Soc. 69*:835–836 (1992).

[Received August 20, 1996; accepted February 3, 1997]